Baghdad Science Journal

Volume 22 | Issue 7 Article 1

7-16-2025

Fabrication of Dye-Sensitized Solar Cell Using CuO Nanoparticles as a Photo anode

Ahmed Mahdi Rheima
Department of Chemistry, College of Science, Mustansiriyah University, Baghdad, Iraq,
ahmed.rheima@uomustansiriyah.edu.iq

Athra G. Sager
Department of Chemistry, College of Science, Wasit University, Wasit, Iraq, asaker@uowasit.edu.iq

Mahdi A. Mohammed
Department of Physics, College of Science, Wasit University, Wasit, Iraq, mahmed@uowasit.edu.iq

Ali Jafer Mahdi
College of Information Technology Engineering, Al-Zahraa University for Women, Karbala, Iraq,
ali.j.mahdi@alzahraa.edu.iq

How to Cite this Article

Rheima, Ahmed Mahdi; Sager, Athra G.; Mohammed, Mahdi A.; and Mahdi, Ali Jafer (2025) "Fabrication of Dye-Sensitized Solar Cell Using CuO Nanoparticles as a Photo anode," *Baghdad Science Journal*: Vol. 22: Iss. 7, Article 1.
DOI: https://doi.org/10.21123/2411-7986.4981

BAGHDAD SCIENCE JOURNAL 2025;22(7):2133–2143

RESEARCH ARTICLE

Fabrication of Dye-Sensitized Solar Cell Using CuO Nanoparticles as a Photo anode

Ahmed Mahdi Rheima [1], **Athra G. Sager** [2,*], **Mahdi A. Mohammed** [3], **Ali Jafer Mahdi** [4]

[1] Department of Chemistry, College of Science, Mustansiriyah University, Baghdad, Iraq
[2] Department of Chemistry, College of Science, Wasit University, Wasit, Iraq
[3] Department of Physics, College of Science, Wasit University, Wasit, Iraq
[4] College of Information Technology Engineering, Al-Zahraa University for Women, Karbala, Iraq

ABSTRACT

Nanoparticles of copper oxide (CuO) are synthesized using a photolysis process. x-ray diffraction (XRD]) is utilized to investigate CuO nanoparticle's crystal structure, and transmission electron microscopy (TEM) is employed to analyze the morphology and the average nanoparticle diameters. Results indicated that the CuO nanoparticles have a monoclinic shape with a mean size of 14 nm. The UV – Visible measurement is shown that the bandgap of CuO nanoparticles is 1.61 eV. The CuO nanoparticles were applied in a photoanode section to fabricate photo organic sensitizer solar cells. The 4,4′-((3,3′-dimethyl-[1,1′-biphenyl]-4,4′-diyl)bis(azaneylylidene))bis (methaneylylidene)) bis (2-methoxy-phenol) was synthesized via the Microwave irradiation method and used as an organic dye sensitizer with different concentrations for solar cells. The highest energy conversion efficiency of the devices was approved to be 10.3% by (ITO/CuO nanoparticles/photo organic sensitizer/iodine/Ag film/ITO).

Keywords: CuO, Nanoparticles, Organic dye, Photolysis, Solar cell

Introduction

Besides the development of supercapacitor[1,2] and battery,[3] the development of solar energy rapidly becomes an important source of renewable energy as an alternative to other traditional sources. While solar cells are recorded to be very efficient, all of these cells are built on a laboratory basis using often rare or costly materials. Research challenges include the costly photovoltaic modules and the provision of a significant portion of energy.[4–6]

The main photovoltaic (PV) materials currently on the market are silicone. However, the "dye sensitization" in solar cells is one of the most attractive methods in the development of solar radiation conversion in the form of electricity at a low cost and high performance.[7,8] A dye sensitized solar cell (DSSC) is a type of the third generation of solar cells that is silicon-free. No high pure material and fairly low cost of production is needed for the DSSC. It contains four major components that affect the activity of cells: photo anodes, photosensitizers, counter electrodes, and electrolytes.[9] Nevertheless, the design and use of DSSCs, including long-term sustainability, degradation, low output, etc, face several challenges. These four components are a key role to enhance DSSC's performance. The selection of dye, which is a part of the photosensitizer component, is a key element. In 1887, the first photosensitization of organic dye was recorded. the chemical compound (tris(2,2′-bipyridyl-4,4′-carboxylate)ruthenium (II) (N3 dye) was known to be the standard dye of classical DSSC.[10]

Received 24 December 2023; revised 15 March 2024; accepted 17 March 2024.
Available online 16 July 2025

* Corresponding author.
E-mail addresses: ahmed.rheima@uomustansiriyah.edu.iq (A. M. Rheima), asaker@uowasit.edu.iq (A. G. Sager), mahmed@uowasit.edu.iq (M. A. Mohammed), ali.j.mahdi@alzahraa.edu.iq (A. J. Mahdi).

https://doi.org/10.21123/2411-7986.4981

Commercialized DSSC and modules using ruthenium bipyridyl-based dyes (N3 dyes or N917) reached a conversion efficiency of more than 10 percent.[11] Such dyes and those chemically produced are however difficult to maintain and costly.[12] Therefore, many researchers are looking forward to developing new dye sensitizers by considering efficiency and cheap materials. Moreover, there are ongoing efforts for the electrode to explore new materials, such as Nanocrystalline semiconductor particles that keep DSSCs stable. The ideal electrode material, such as copper, aluminum, platinum, and tungsten should be capable of high electrical conductivity, excellent chemical and physical constancy, efficient catalytic operation, resistance to corrosion and affordability.[13]

The photoanodes are nanocrystal semiconductors. Copper oxide (CuO) is one of many materials that can be used as photoanodes in DSSC. CuO has intensive priorities and was reviewed thoroughly for its distinguishing properties in the various transition metals semiconductor oxides. CuO is a p-type semiconductor and is considered to have a small bandgap (E_g) in the range from 1.2 to 1.4 eV and the monoclinic structure of a crystal, making it a promising product for gas sensors, magnetic storage, solar cells, electronics, semiconductors, varistors and catalysts.[13,14] Many researchers studied the CuO-based p-type DSSCs. The obtained efficiencies were found to be 3.4%,[15] 2.963%,[16,17] 1.7%[18] and 0.5.%[19] The variation of efficiencies was due to the type of organic dye and the method of CuO synthesis that affects the particle size, morphology and crystallinity. For example, Langmar et al.,[20] found the efficiencies of commercial and synthesized CuO nanoparticles that were used as photocathodes were 0.073% and 0.11%, respectively. The efficiency increased because the synthesized CuO nanoparticles were smaller than commercial ones which enable higher dye loading. Moreover, other researchers studied CuO as a composite with other nanoparticles such as TiO_2, which obtained efficiencies of 7.73%.[21]

The nanomaterials have unique characterizations and have been studied in different applications.[22–24] Size and shape constitute a significant determinant of the packaging of nanocrystal atoms on the top or the exposed side.[25] Because of its inexpensive, easy to access and high conductance, copper represents a good alternative precursor for copper nanoparticles (CuO-NPs) synthesis.[26] The CuO-NPs can be synthesized using various methods including electrochemical approach,[27] laser ablation method,[28] microwave method,[29] hydrothermal process,[30] colloidal gas aphron,[31] solvothermal method,[32] Sonochemical method[33] and ball milling.[34] However, several drawbacks come with these methods including the unnecessary usage and hazardous reagents, high temperatures and pressures, multistage synthesis, additional capping agents, use of costly reagents ($NaBH_4$ and PVP), response time, the need for specialized instruments and the needs during the reaction for external additives. The design of simple, stable, cost-effective and convenient methods for copper oxide syntheses nanoparticles is therefore important which overcomes these drawbacks.

In the current study, the synthesis of CuO NPs is done by the photolysis method which is used UV-irradiation as a source for the first time. This method is easy to set and use, efficient and low cost. Because the properties of nanoparticles change when their sizes are decreased, the CuO NPs are used as a photoanode in this study to determine their efficiency in DSSC. Moreover, the organic dye was papered to use as a photosensitizer in the solar cell.

Materials and methods

Materials

Copper(II)chloride (99%, blue), Urea (99%, White), Vanillin (99%, yellow), ethanol (99.9%),o-toluidine (99.9%, green) was purchased from Sigma-Aldrich. The chemical products were analytical grades of reagents and were used without a purification process.

Synthesis of CuO NPs

The spherical nanoparticles of CuO were synthesized by a photolysis process.[35] The photocell kits contain a UV source of a mercury lamp with a power of 125 W that has a 365 nm wavelength of light intensity, and the reactor tube of Pyrex was cooled to prevent an increase in temperature due to the UV irradiation by ice bath. 25 ml of 0.1M copper chloride $CuCl_2$ was mixed with 25 ml of 0.1M of urea using deionized water as a solvent. The mixture was irradiated for half an hour. The produced (precipitate) was separated and washed five times using deionized water in a centrifuge. The black precipitate of CuO -NPs was obtained while drying the material overnight and calcining it in an oven at 400°C for three hours.

Synthesis of 4,4,-((3,3,-dimethyl-[1,1,-biphenyl]-4,4,-diyl)bis(azaneylylidene))bis(methaneylylid ene)bis (2-methoxy-phenol) (A).

The compound A was synthesized via microwave irradiation method as shown in Scheme 1. (0.01 mol, 1.521 g) of vanillin was dissolved in 10 ml of ethanol. The obtained solution was acidity with three drops

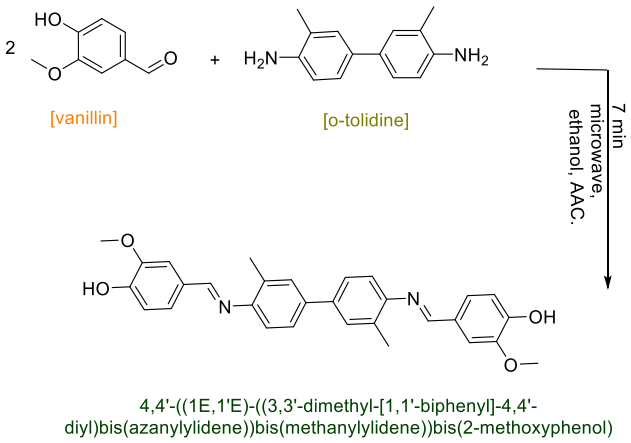

Scheme 1. The procedure used tosynthesize the compound A.

of glacial acetic acid. Then, O-Tolidine (0.005 mol, 1.061g) was mixed with the obtained solution.[36] The mixture was irradiated by using a microwave at 300 Wt. for seven minutes. The precipitate was cooled by using an ice bath for 2 hours. The green participate was separated and washed with cold ethanol several times and diethyl ether. Finally, it was dried in the vacuum oven at 50°C. The yield of the compound is 90.01 %, 153.5°C melting point, and 480.56 Molecular Weight: Anal.Found for $C_{30}H_{28}N_2O_4$ (%): C, 74.9; H, 5.78; N, 5.84. Calc. C, 74.93; H, 5.79; N,5.83. The compound was characterized by FT-IR spectroscopy and ^{1}H-^{13}CNMR.

The preparation of photo organic sensitizer solar cell (POSSC)

The Indium-doped tin oxide (ITO) is resistant at 8 ohms and 83% transmission and coated glass was washed sundry times with ethanol and de-ionized water by using an ultrasonic bath. Then it was dried using an air blower. A photo organic sensitized solar cell (20 × 15 × 1 mm) was fabricated according to the following steps:

First step: The colloidal solution of CuO-NPs was synthesized by adding (0.2 g) of the nanoparticle powder with absolute ethanol of 15 mL. The photoanode was gained by using a dropper to cover the conductive side of the glass with the colloidal solution, thereafter annealed at (200°C) for 1 hour in the air.

The Second step: The CuO-NPs electrode was cooled at room temperature, then it was immersed overnight in the different concentrations (0.001, 0.005, 0.01, and 0.1 M) of compound A that were dissolved in ethanol.

Third step: The nano-film silver (Ag) was coated on the conductive side of the glass to use as a counter electrode.

Finally step: The photo-anode (sensitized nanoparticles of CuO) and the counter electrode coated with nano-film silver (Ag) was assembled and the liquid electrolyte (I^{-}/I^{-3}) solution penetrated by capillary action into the working space and counter electrode.

Characterization

The powder of CuO was characterized by using (Shimadzu XRD-6000, Japan). The X-ray diffractometer was operated at 30 mA and 40 Kv to generate radiation at a wavelength of 1.5406 Å. The size and morphology of nanoparticles were measured using TEM (JEOL JEM-2100, Japan). The absorbance of CuO NPs was measured by UV-Visible spectrometer (Shimadzu 160 V, Japan). The infrared spectra were determined by using KBr pressed disc method on a (Thermo FT-IR-8300, USA). FT-IR spectrophotometer was measured in the range of 4000–400 cm^{-1}. Micro elemental analysis CHN were obtained on a Perkin-Elmer Model 2400 CHNS, USA elemental analyzer. ^{1}H -^{13}C NMR was recorded spectra on a (Bruker Ultra shield 400MHz, USA) spectrometer using DMSOd[6] as the solvent, with tetramethylsilane as an internal reference.

Results and discussion

The analysis of XRD was performed to know the crystalline structure and quality. Fig. 1 displays the XRD pattern of prepared of CuO nanoparticles. The pattern supports the crystalline structure of the monoclinic. All the peaks at diffraction angles (2Theta) in the region of 32.7°, 35.8°, 38.7°, 48.7°, 53.5°, 58.3° correspond to 110, 002, 111, –202, 020, 202 phases for the CuO nanoparticles. The peak positions are shown to be very much in line with the recorded values (JCPDS) and they agree with references.[37]

TEM was carried out to obtain the quantitative analysis of particle/grain size, distribution of dimensions and morphology. Fig. 2 shows the TEM images of synthesized CuO nanoparticles. The particles are spherical and well dispersed. This means the CuO nanoparticles are highly crystalline and have good morphology because a key factor controlling the morphology and structure of the final output is particle aggregation.[38] Fig. 2 shows, the particle size (average) was found to be 14 nm.

The diffuse reflection spectrum of UV-Vis was used in the determination of the optical characteristics of synthesized CuO nanoparticles. Fig. 3a shows the

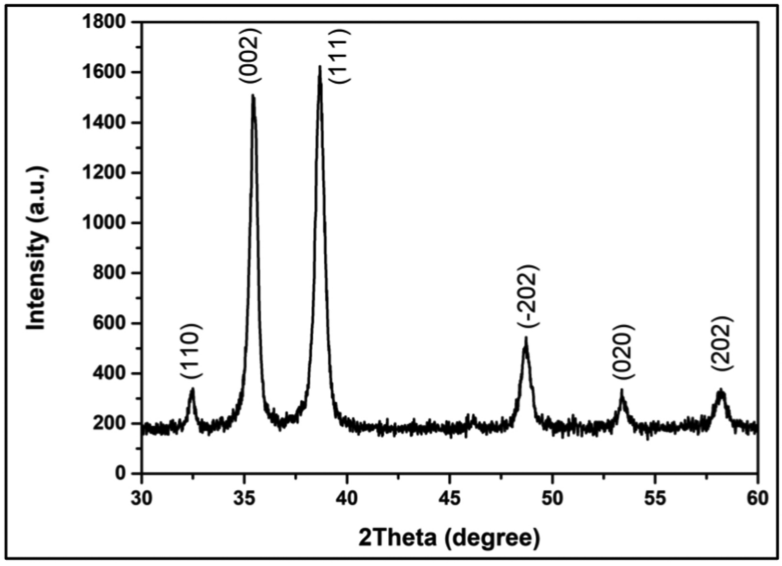

Fig. 1. XRD patterns of the CuO-NPs.

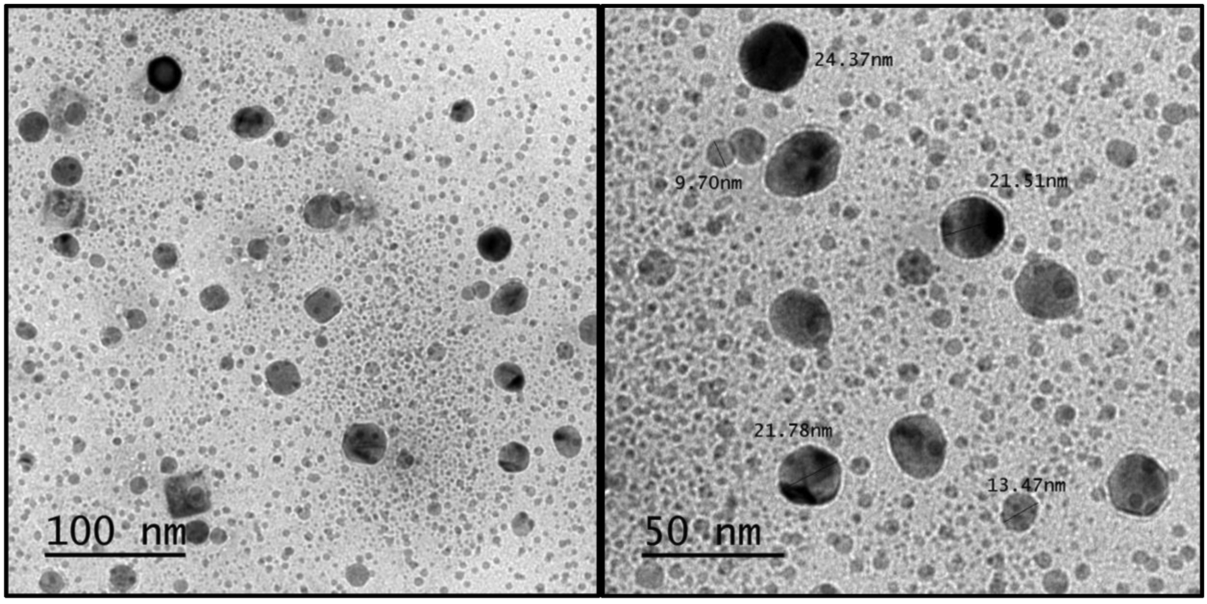

Fig. 2. TEM images of the CuO nanoparticles at different scale sizes (100 and 50 nm).

absorption spectra of CuO nanoparticles. The optical properties of CuO nanoparticles have clear absorption for visible light. The edge of absorption is used to determine the type of transition and bandgap value. The bandgap of CuO nanoparticles was calculated using the Tauc Eq. (1):[39]

$$(\alpha h\nu)^2 = \mathrm{A}\,(h\nu - E_g) \quad (1)$$

where: The energy of the optical bandgap (E_g), Planks constant (h), Absorbance (α), Frequency of incident radiation = ν, and A refers to band tailing parameter (constant).

Fig. 3b shows the relationship between $(\alpha h\nu)^2$ and the band gap for CuO nanoparticles. By extrapolating the linear part to the energy of the optical bandgap axis, the E_g value can be determined. The direct bandgap value was found to be 1.61 eV which is much greater than the recorded value of bandgap of bulk CuO (1.4 eV) because of quantum confinement which is due to an aspect ratio of the nanoparticles.[40]

The FT-IR data that comes from FT-IR spectrum shows the major significant band (O-H) at 3350 cm^{-1}. It is shown to have an aromatic ring by the presence of the band following at 3073 cm^{-1} assignable to aromatic_H stretching vibration.[41] 2981 (C-H

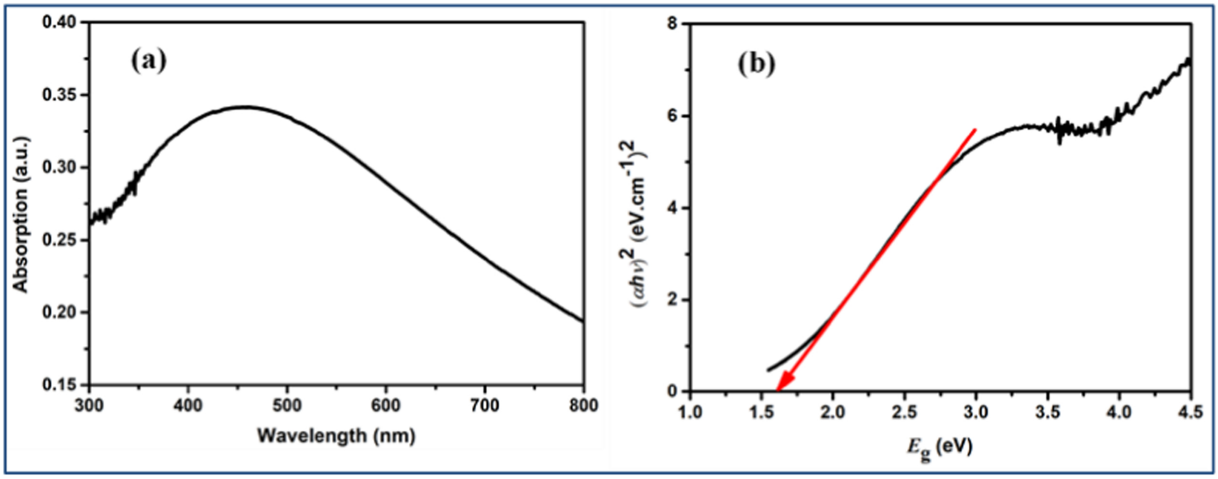

Fig. 3. (a) Absorption spectrum of CuO nanoparticles in the visible range. (b) Plot of $(\alpha h\nu)^2$ versus the energy of bandgap for CuO nanoparticles.

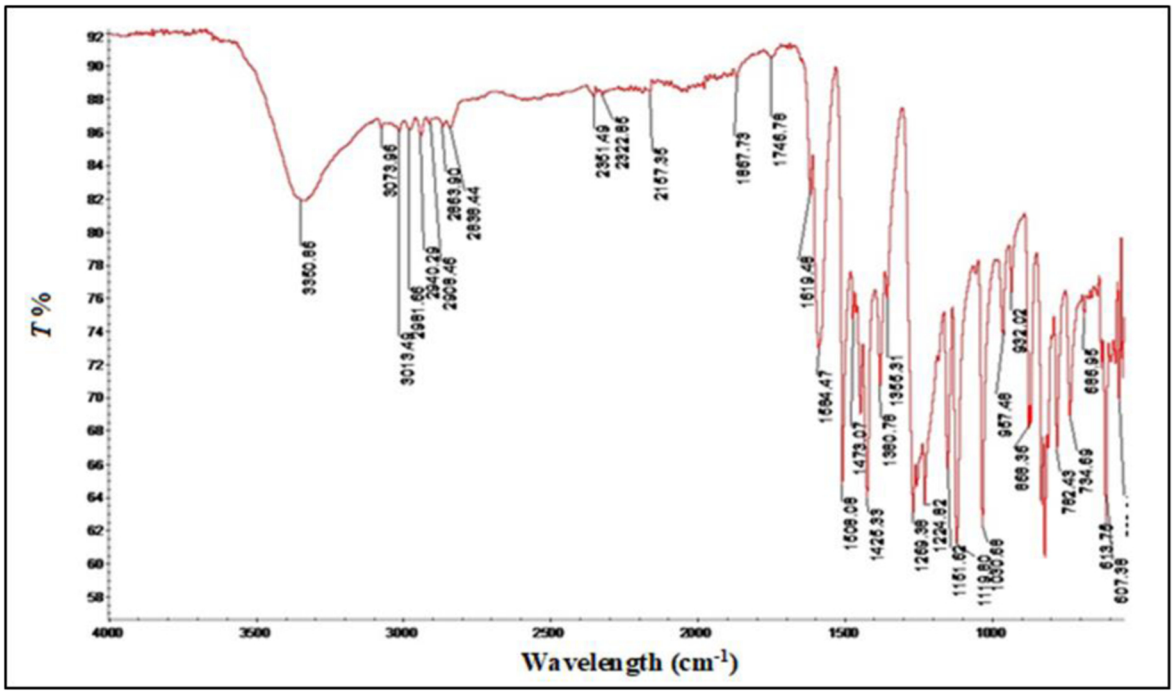

Fig. 4. The FT-IR spectrum of an organic compound A.

aliphatic), on the other hand, is the highest intensity at 1619 cm^{-1} can be attributed to the amine group (C=N).[42,43] The strong band was shown at the frequency of 1584 cm^{-1} that can be assigned to the stretching of (C=C). The bond at 1426 cm^{-1} is due to stretching ν(C-O) group in OCH3 and the bonds at 1161 and 1224 cm^{-1} was attributed to stretching vibration of ν(C-N) groups.[42] Fig. 4 shows the IR spectrum of a compound.

^{1}H-NMR [DMSO-d$_6$,TMS]: δppm = 2.47 (s, 6H,alphalic) for methy, δppm = 3.82 (s, 6H,alphalic) for methoxy, 6.871 ppm (d, 2H, aromatic proton H), 7.27–7.71ppm (m, 10 H, aromatic proton) for the rings, 8.57 ppm (s,1H, imine) and 8.65 ppm (s, 1H,imine). 9.42 ppm (s, 2H,O-H). The ^{1}H-NMR spectrum of a compound A is illustrated in Fig. 5.

The ^{13}C NMR spectrum of organic compound Scheme.2 is shown in Fig. 6. ^{13}C NMR [δppm]: The presence of the atom carbon for the imine group (HC=N) is attributed from the peak at δ = 158.4.[44] The presence of the atom carbon for CH_3 was shown in the range of δ = 18.8, and the presence of the atom

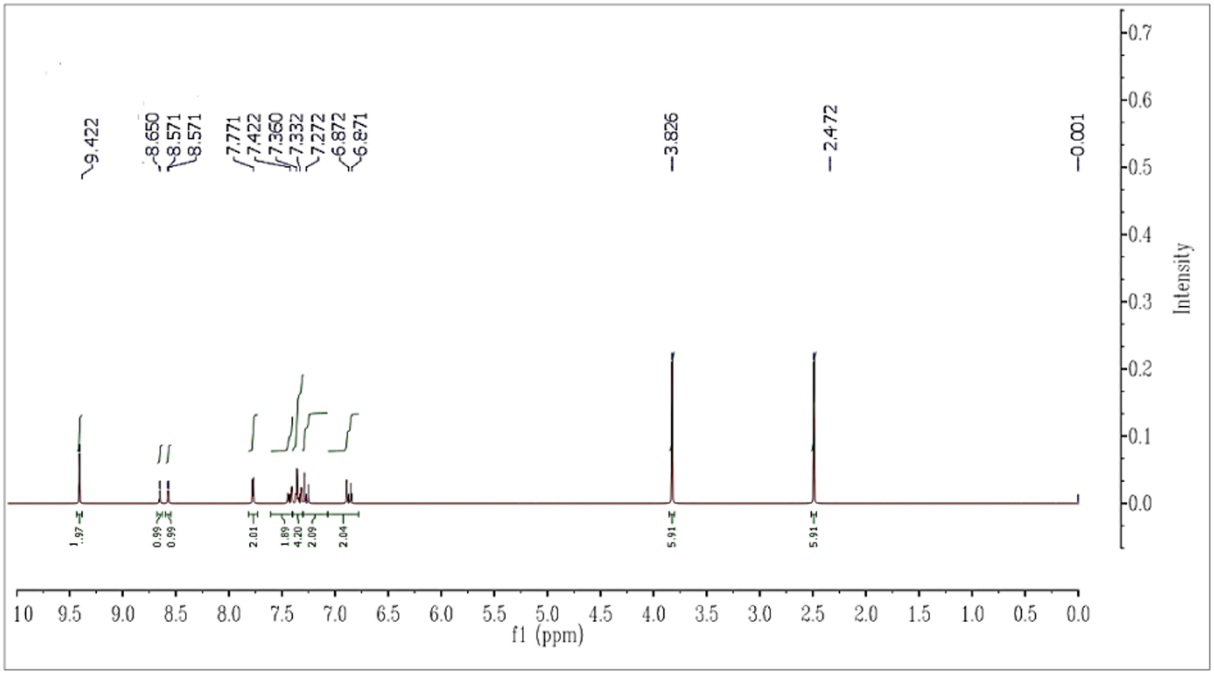

Fig. 5. ^{1}H NMR spectrum of an organic compound at 400 MHz.

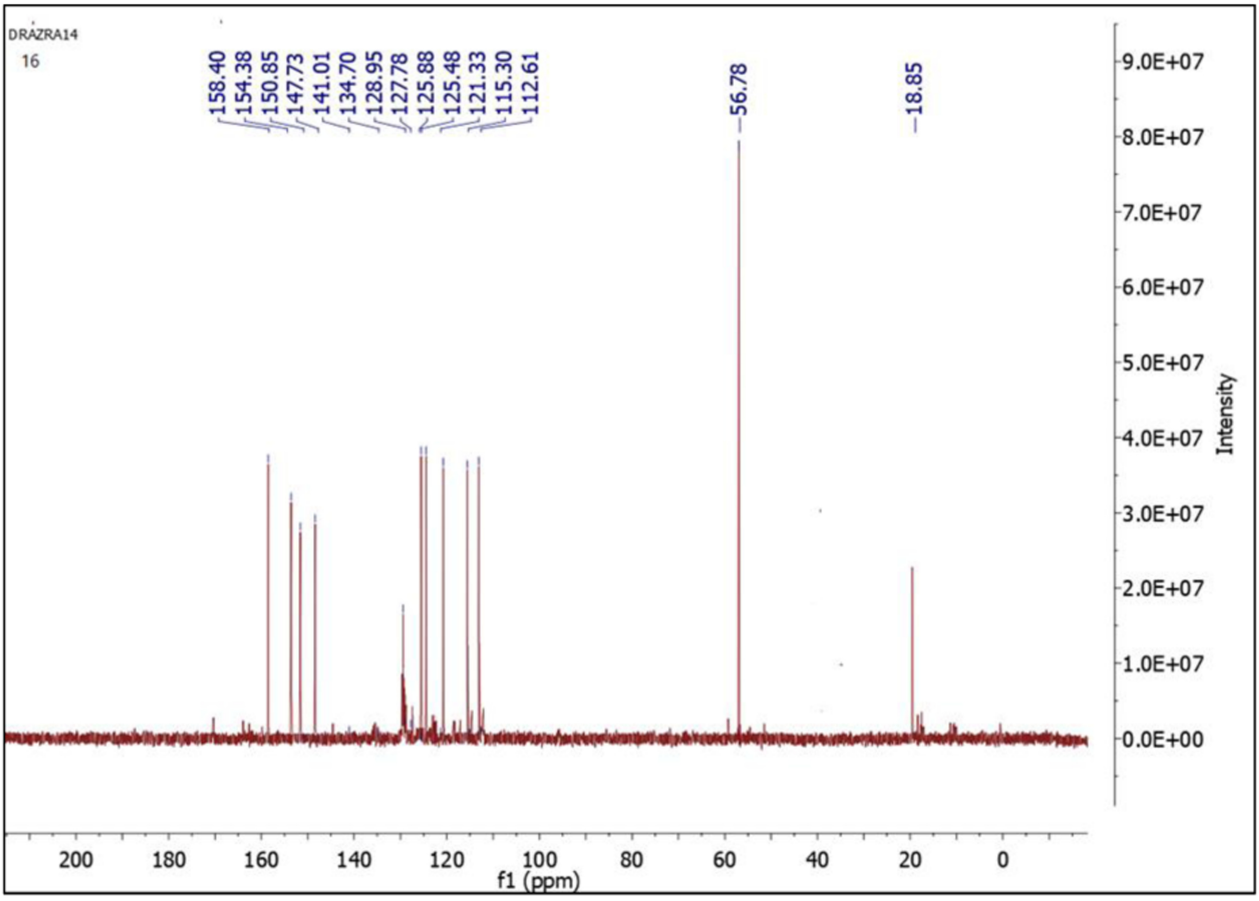

Fig. 6. ^{13}C NMR spectrum of the organic compound.

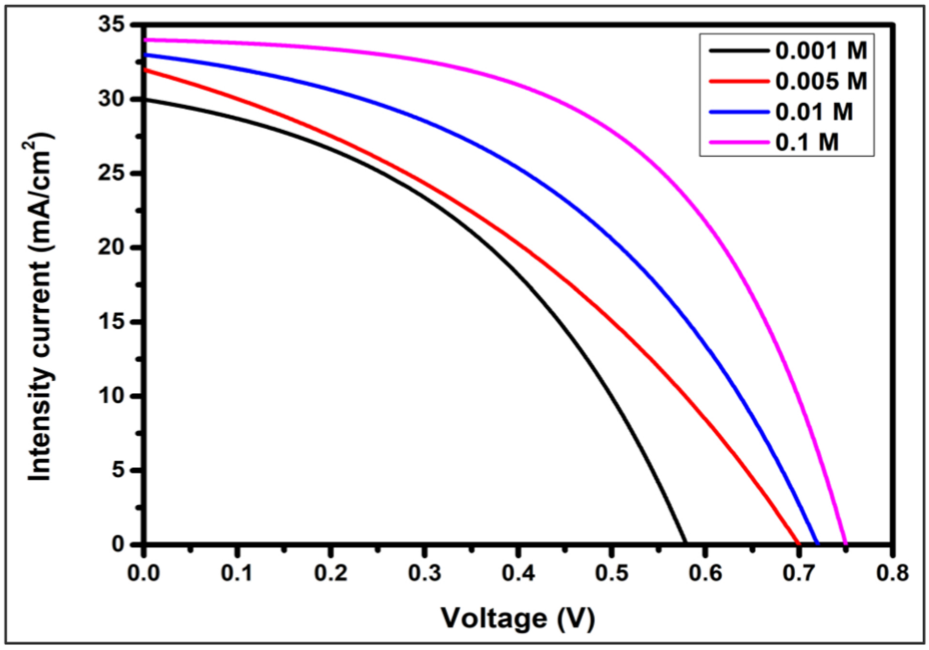

Fig. 7. Photovoltaic properties of the DSSC.

Table 1. The parameters of organic sensitizer solar cell: (ITO/CuO nanoparticles/photo organic sensitizer/iodine/Ag film/ITO).

The concentration of photo organic sensitizer [M]	V_{oc}(V)	J_{sc} (A/cm^2)	V_{max} (V)	J_{max} (A/cm^2)	P_{max} (W/cm^2)	FF	η
0.001	0.58	0.030	0.34	0.015	0.0051	0.293	5.1%
0.005	0.70	0.032	0.36	0.018	0.0064	0.289	6.47%
0.01	0.72	0.033	0.56	0.017	0.0095	0.400	9.5%
0.1	0.75	0.034	0.61	0.017	0.0103	0.406	10.3%

carbon for OCH_3 was shown in the range of 56.8. The resonances because of the aromatic carbon atoms in each of the rings of the synthesized compound can be placed on the chemical shift in the range of δ =154.3–112.61.

^{13}CNMR δppm: 158.4 of (CH=N), 18.85 of methyl group 56.8 of methoxy group, 112.6–154.3 carbons aromatic rings.[45]

Fig. 7 displayed the photovoltaic properties of DSSCs based on CuO nanoparticles as a photoelectrode with different concentrations of organic compounds as a photosensitizer. A solar simulator consists of an organic solar cell that was illuminated by a halogen lamp with an intensity of 100 mW/cm^2. The efficiency of solar cell power conversion was measured by Eq. (2):[46]

$$\eta = \frac{P_{max}}{P_{in}} = \frac{V_{OC} \cdot J_{SC} \cdot FF}{P_{in}} \times 100\ \% \quad (2)$$

where:

V_{OC}, J_{SC} and P_{in} represent the open-circuit photovoltage, the photocurrent of short-circuit density and the power of incident light, respectively. The fill factor is described by:

$$FF = \frac{V_{max} \cdot J_{max}}{V_{OC} \cdot J_{SC}} \quad (3)$$

where:

V_{max} is the voltage maximum output power.

J_{max} is the current density at the maximum output power.

With increasing the organic concentrations, the power conversion efficiency of the cells was increased. In more details, Table 1 shows the list of the photoelectric characterization including V_{oc}, J_{sc}, V_{max} and J_{max} and FF. A huge difference in photoelectric parameter values is shown when the organic concentration was increased to 0.01 M under the same conditions. However, the values were not changed noticeably with increasing the organic concentration of more than 0.01 M. It was displayed that our DSSC with photosensitizer concentration 0.1 M had the highest short circuit current and high open-circuit voltage. This is because of the molecular structure

of CuO nanoparticles (favorable for the separation of electron/hole pairs) with the diffusion rate of redox electrolyte phase, increased sensing and absorption of light by the organic compound. The result shows the highest efficiency incomparable with the results in the literature review.[47]

Conclusion

The CuO nanoparticles were synthesized successfully by a simple, affordable and efficient photolysis approach. A micrographic analysis observed the distribution of spherical CuO NPs and the mean particle diameter was measured to be 14 nm through TEM measurement. The UV absorption was used to analyze the optical characteristics of CuO nanoparticles. The direct optical bandgap of CuO NPs, which was 1.61 eV, was shown to be bigger than the bulk material due to the quantum confinement of nanoparticles. The efficiency of the organic dye was directly proportional to its concentrations. It was shown to have maximum efficiency at 10.3% with a 0.1 M concentration.

Acknowledgments

This work was supported by the Ministry of Higher Education and Scientific Research, Baghdad, Iraq.

Author's declaration

- Conflicts of Interest: None.
- We hereby confirm that all the figures and tables in the manuscript are ours. Besides, the figures and images, which are not ours, have been given the permission for re-publication attached with the manuscript.
- No animal studies are present in the manuscript.
- No human studies are present in the manuscript.
- Ethical Clearance: The project was approved by the local ethical committee at Waist University.

Author's contribution

A. M. R. contributed to the design and implementation of the study and the analysis of the results. A. G. S. contributed to analyzing the data. M. A. M. and A. J. M. contributed to the writing of the manuscript. All authors have read and agreed to the final draft of the manuscript.

References

1. Duan P, Yang S, He P, Zhang P, Xie X, Ding G. Coordinating capillary infiltration with anodic oxidation: A multi-functional strategy for electrochemical fabrication of graphene. RSC Adv. 2020;10(71):43324–43333. https://doi.org/10.1039/d0ra07531k.
2. Ji S, Yang J, Cao J, Zhao X, Mohammed MA, He P, *et al.* A universal electrolyte formulation for the electrodeposition of pristine carbon and polypyrrole composites for supercapacitors. ACS Appl Mater Interfaces. 2020;12(11):13386–13399. https://doi.org/10.1021/acsami.0c01216.
3. Alwash A. The green synthesize of zinc oxide catalyst using pomegranate peels extract for the photocatalytic degradation of methylene blue dye. Baghdad Sci J. 2020;17(3):787–794. https://doi.org/10.21123/bsj.2020.17.3.0787.
4. Fara L, Chilibon I, Craciunescu D, Diaconu A, Fara S. Review: Heterojunction tandem solar cells on Si-based metal oxides. Energies. 2023;16(7):3033. https://doi.org/10.3390/en16073033.
5. Almomani MS, Ahmed NM, Rashid M, Ibnaouf KH, Aldaghri OA, Madkhali N, *et al.* Performance improvement of graded bandgap solar cell via optimization of energy levels alignment in Si quantum dot, TiO_2 nanoparticles, and porous Si. Photonics. 2022;9(11):843. https://doi.org/10.3390/photonics9110843.
6. Wang B, Yu S, Huang L. Zinc oxide-encapsulated copper nanowires for stable transparent conductors. Nanomater. 2023;13(19):2659. https://doi.org/10.3390/nano13192659.
7. Rheima, AM, Hussain DH, Abdulah HI. Novel method to synthesis Fe_3O_4 nanoparticles for novel dye solar cell. J Adv Sci Nanotechnol. 2022;1(1):9–19. https://doi.org/10.55945/joasnt.2022.1.1.9-19.
8. Tamarani A, Zainul R, Dewata I. Preparation and characterization of XRD nano Cu-TiO 2 using sol-gel method. Int J Mod Phys Conf Ser. IOP Publishing, 2020; 1185(1):012020. https://doi.org/10.1088/1742-6596/1185/1/012020.
9. Hardeli H, Zainul R, Isara LP. Preparation of dye sensitized solar cell (DSSC) using anthocyanin color dyes from jengkol shell (Pithecellobium lobatum Benth.) by the gallate acid copigmentation. Int J Mod Phys Conf Ser. IOP Publishing, 2021;1185(1):O12021. https://doi.org/10.1088/1742-6596/1185/1/012021.
10. Kassegn GK, Sibhatu AK. Photocatalytic activity of biosynthesized α-Fe_2O_3 nanoparticles for the degradation of methylene blue and methyl orange dyes. Optik. 2021;241:167226. https://doi.org/10.1016/j.ijleo.2021.167226.
11. Nazeeruddin MK, Kay A, Rodicio I, Humphry-Baker R, Mueller E, Liska P. *et al.* Conversion of light to electricity by cis-X2bis (2, 2′-bipyridyl -4, 4′-dicarboxylate) ruthenium (II) charge-transfer sensitizers (X= Cl-, Br-, I-, CN-, and SCN-) on nanocrystalline titanium dioxide electrodes. J Am Chem Soc. 1993;115(14):6382–6390. https://doi.org/10.1021/ja00067a063.
12. Cherepy NJ, Smestad GP, Grätzel M, Zhang JZ. Ultrafast electron injection: implications for a photoelectrochemical cell utilizing an anthocyanin dye-sensitized TiO_2 nanocrystalline electrode. J Phys Chem B. 1997;101(45):9342–9351. https://doi.org/10.1021/jp972197w.
13. Vidyasagar CC, Nayaka YA, Venkatesha TG, Viswanatha R. Solid-state synthesis and effect of temperature on optical properties of CuO nanoparticles. Nano-Micro Lett. 2012;4(2):73–77. https://doi.org/10.3786/nml.v4i2.p73-77.

14. Ahmed KH, Mohammed AA, Imad ML, A green synthesis of Iron/Copper nanoparticles as a catalytic of fenton-like reactions for removal of Orange GDye. Baghdad Sci J. 2022;19(6):1249–1264. https://doi.org/10.21123/bsj.2022.6508.
15. Sharma JK, Akhtar MS, Ameen S, Srivastava P, Singh G. Green synthesis of CuO nanoparticles with leaf extract of Calotropis gigantea and its dye-sensitized solar cells applications. J Alloys Compd. 2015;632:321–325. https://doi.org/10.1016/j.jallcom.2015.01.172.
16. Wanninayake AP, Gunashekar S, Li S, Church CB, Abu-Zahra N. CuO Nanoparticles based bulk heterojunction solar cells: Investigations on morphology and performance. J Sol Energy Eng. 2015;137(3):031016. https://doi.org/10.1115/1.4029542.
17. Hilal HI, Jabbar HR, Muslime HA, Shakir WA. Preparation (PMMA/PVA)-copper oxide nano composites solar cell. AIP Conf Proc. 2020;2290(1):050036. https://doi.org/10.1063/5.0027846.
18. Satish B, Rajendar V, Rao KV, Chakra CS. Enhanced power conversion efficiency of dye synthesized solar cell by few layered graphene/CuO nanocomposite as a working electrode. Dig J Nanomater Biostruct. 2017;12(1):67–72. https://doi.org/10.1039/c9ra03344k.
19. Prabhin VS, Jeyasubramanian K, Romulus NR, Singh NN. Fabrication of dye sensitized solar cell using chemically tuned CuO nano-particles prepared by sol-gel method. Arch Mater Sci Eng. 2017;83(1):5–9. https://doi.org/10.5604/01.3001.0009.7535.
20. Ashir MBA, Rajpar AH, Salih EY, Ahmed EM. Preparation and photovoltaic evaluation of CuO@Zn(Al)O-mixed metal oxides for dye sensitized solar cell. Nanomater. 2023;13(5):802. https://doi.org/10.3390/nano13050802.
21. Beedri NI, Dani G, Gaikwad M, Pathan HM, Salunke-Gawali S. Comparative study of TiO_2, ZnO, and Nb_2O_5 photoanodes for nitro-substituted naphthoquinone photosensitizer-based solar cells. ACS Omega. 2023 Oct 2;8(41):38748–38765. https://doi.org/10.1021/acsomega.3c06271.
22. Enea N, Ion V, Viespe C, Constantinoiu I, Bonciu A, Stîngescu ML, *et al.* Lead-free perovskite thin films for gas sensing through surface acoustic wave device detection. Nanomater. 2024;14(1):39. https://doi.org/10.3390/nano14010039.
23. Sadique MA, Yadav S, Khare V, Khan R, Tripathi GK, Khare PS. Functionalized titanium dioxide nanoparticle-based electrochemical immunosensor for detection of SARS-CoV-2 antibody. Diagnostics. 2022;12(11):2612. https://doi.org/10.3390/diagnostics12112612.
24. Min Y, Suminda GGD, Heo Y, Kim M, Ghosh M, Son Y-O. Metal-based nanoparticles and their relevant consequences on cytotoxicity cascade and induced oxidative stress. Antioxidants. 2023;12(3):703. https://doi.org/10.3390/antiox12030703.
25. Bagheri FH, Khabazzadeh H, Fayazi M. Rezaeipour M. Synthesis of CuO and Cu_2O nanoparticles stabilized on the magnetic Fe_3O_4-Montmorillonite-K10 and comparison of their catalytic activity in A3 coupling reaction. J Iran Chem SOC. 2023;20:1439–1456. https://doi.org/10.1007/s13738-023-02768-z.
26. Zhu Z, Xia H, Jiang J, Han S, Li H. Ultrasound-assisted hydrothermal synthesis of $SrSnO_3$/g-C_3N_4 heterojunction with enhanced photocatalytic performance for ciprofloxacin under visible light. Crystals. 2022;12(8):1062. https://doi.org/10.3390/cryst12081062.
27. Prabu P, Losetty V. Green synthesis of copper oxide nanoparticles using Macroptilium Lathyroides (L) leaf extract and their spectroscopic characterization, biological activity and photocatalytic dye degradation study. J Mole Stru. 2024 April 5;1301:137404. https://doi.org/10.1016/j.molstruc.2023.137404
28. Hesabizadeh T, Sung K, Park M, Foley S, Paredes A, Blissett S, *et al.* Synthesis of antibacterial copper oxide nanoparticles by pulsed laser ablation in liquids: Potential application against foodborne pathogens. Nanomater. 2023;13(15):2206. https://doi.org/10.3390/nano13152206.
29. Rajamohan R, Raorane CJ, Kim S-C, Ashokkumar S, Lee YR. Novel microwave synthesis of copper oxide nanoparticles and appraisal of the antibacterial application. Micromachines. 2023;14(2):456. https://doi.org/10.3390/mi14020456.
30. Dharmana G, Gurugubelli TR, Masabattula PSR, Babu B, Yoo K. Facile synthesis, characterization, and photocatalytic activity of hydrothermally grown Cu^{2+}-Doped ZnO–SnS nanocomposites for MB dye degradation. *Catalysts*. 2022;12(3):328. https://doi.org/10.3390/catal12030328.
31. Demel J, Zhigunov A, Jirka I, Klementová M, Lang K. Facile synthesis of CuO nanosheets via the controlled delamination of layered copper hydroxide acetate. J Colloid Interface Sci. 2015;452:174–179. https://doi.org/10.1016/j.jcis.2015.04.023.
32. Aljedaani RO, Kosa SA, Abdel Salam M. Ecofriendly green synthesis of Copper(II) oxide nanoparticles using corchorus olitorus leaves (Molokhaia) extract and their application for the environmental remediation of direct violet dye via advanced oxidation process. Molecules. 2023;28(1):16. https://doi.org/10.3390/molecules28010016.
33. Moura AP, Cavalcante LS, Sczancoski JC, Stroppa DG, Paris EC, Ramirez AJ, *et al.* Structure and growth mechanism of CuO plates obtained by microwave-hydrothermal without surfactants. Adv Powder Technol. 2010;21(2):197–202. https://doi.org/10.1016/j.apt.2009.11.007.
34. Dubadi R, Huang SD, Jaroniec M. Mechanochemical synthesis of nanoparticles for potential antimicrobial applications. Mater. 2023;16(4):1460. https://doi.org/10.3390/ma16041460.
35. Khan SA, Shahid S, Hanif S, Almoallim HS, Alharbi SA, Sellami H. Green synthesis of chromium oxide nanoparticles for antibacterial, antioxidant anticancer, and biocompatibility activities. Int J Mol Sci. 2021;22(2):502. https://doi.org/10.3390/ijms22020502.
36. Crisan CM, Mocan T, Manolea M, Lasca LI, Tăbăran F-A, Mocan L. Review on silver nanoparticles as a novel class of antibacterial solutions. Appl Sci. 2021;11(3):1120. https://doi.org/10.3390/app11031120.
37. Al-Redha HMA, Ali SH, Mohammed SS. Syntheses, structures and biological activity of some schiff base metal complexes. Baghdad Sci J. 2022;19(3):0704. https://doi.org/10.21123/bsj.2022.19.3.0704.
38. Keabadile OP, Aremu AO, Elugoke SE, Fayemi OE. Green and traditional synthesis of copper oxide nanoparticles—comparative study. Nanomater. 2020;10(12):2502. https://doi.org/10.3390/nano10122502.
39. Aroussi S, Dahamni MA, Ghamnia M, Tonneau D, Fauquet C. Characterization of some physical and photocatalytic properties of CuO nanofilms synthesized by a gentle chemical technique. Condens Matter. 2022;7(2):37. https://doi.org/10.3390/condmat7020037.
40. Madona J, Sridevi C, Velraj G, Raj DA, George A. Surfactant assisted morphology controlled CuO nanostructures for enhanced photocatalytic performance and bacterial growth inhibition. Mater Sci Eng. 2023;August;294:116562. https://doi.org/10.1016/j.mseb.2023.116562.

41. Amin MF, Gnida P, Kotowicz S, Małecki JG, Siwy M, Nitschke P, Schab-Balcerzak E. Spectroscopic and physicochemical investigations of azomethines with triphenylamine core towards optoelectronics. Materials. 2022;15(20):7197. https://doi.org/10.3390/ma15207197.
42. Athra G S, Athraa HM. Synthesis and characterization new liquid crystals of Schiff base using microwave radiation. *Drug Invent Today*, 2020;14(1):70–78.
43. Limosani F, Tessore F, Forni A, Lembo A, Di Carlo G, Albanese C, *et al.* Nonlinear optical properties of Zn(II) porphyrin, graphene nanoplates, and ferrocene hybrid materials. Materials. 2023;16(15):5427. https://doi.org/10.3390/ma16155427.
44. Sager A G, Abaies JK, Katoof ZR. Molecular docking, synthesis and evaluation for antioxidant and antibacterial activity of new oxazepane and benzoxazepine derivatives. Baghdad Sci J. 2023;24(7):8822–8037 https://dx.doi.org/10.21123/bsj.2023.8553.
45. Sulistyowaty MI, Uyen NH, Suganuma K, Chitama BA, Yahata K, Kaneko O, Sugimoto S, *et al.* Six new phenylpropanoid derivatives from chemically converted extract of alpinia galanga (L.) and their antiparasitic activities. Molecules. 2021;26(6):1756. https://dx.doi.org/10.3390/molecules26061756.
46. Lai F-I, Yang J-F, Chen W-C, Hsu Y-C, Kuo S-Y. Enhancing dye-sensitized solar cell performance with different sizes of ZnO nanorods grown using multi-step growth. *Catalysts*. 2023;13(9):1254. https://doi.org/10.3390/catal13091254.
47. Mehrabian M, Taleb-Abbasi M, Akhavan O. Using Cu_2O/ZnO as two-dimensional hole/electron transport nanolayers in unleaded FASnI3 perovskite solar cells. Materials. 2024;17(5):1064. https://doi.org/10.3390/ma17051064.

تصنيع خلية شمسية حساسة للصبغة باستخدام جسيمات النحاس النانوية كأنود ضوئي

احمد مهدي رحيمة [1]، عذراء كظامي صكر[2]، مهدي احمد محمد[3]، علي جعفر مهدي[4]

[1]قسم الكيمياء، كلية العلوم، جامعة المستنصرية، بغداد، العراق.
[2] قسم الكيمياء، كلية العلوم، جامعة واسط, واسط، العراق.
[3] قسم الفيزياء، كلية العلوم، جامعة واسط، واسط، العراق
[4] كلية هندسة تكنولوجيا المعلومات، جامعة الزهراء للبنات، كربلاء، العراق.

الخلاصة

يتم تصنيع الجسيمات النانوية لأكسيد النحاس (CuO) باستخدام عملية التحلل الضوئي. وتم استخدام حيود الأشعة السينية XRD لفحص البنية البلورية لجسيمات النحاس النانوية، ويستخدم المجهر الإلكتروني النافذ (TEM) لتحليل التشكل ومتوسط أقطار الجسيمات النانوية. تشير النتائج إلى أن الجسيمات النانوية CuO لها شكل أحادي الميل بمتوسط حجم 14 نانومتر. ,يظهر القياس المرئي للأشعة فوق البنفسجية أن فجوة نطاق جسيمات النحاس النانوية تبلغ 1.61 فولت. تم تطبيق الجسيمات النانوية CuO في قسم الأنود الضوئي لتصنيع الخلايا الشمسية المحسسة للضوء العضوي. المركب 4,4'-((3,3'-ثنائي ميثيل-[1,1'-ثنائي الفينيل]-4,4'-دييل) تنائي(أزانيليدين)) تنائي (ميثانيليليدين)) ثنائي (2-ميثوكسي-فينول) تم تصنيعه بطريقة التشعيع باستخدام الميكروويف واستخدم المركب كمحسس صبغة عضوية بتراكيزمختلفة للخلايا الشمسية. تم اعتماد أعلى كفاءة تحويل للطاقة في الأجهزة بنسبة 10.3% بواسطة (ITO/CuO nanoparticles/photoorganic ensitizer/iodine/Ag film/ITO).

الكلمات المفتاحية:. اوكسيد النحاس، الجسيمات النانوية، الصبغة العضوية، التحلل الضوئي، الخلايا الشمسية.